Springer

KSME

Journal of Mechanical Science and Technology 33 (3) (2019) 1311~1319
www.springerlink.com/content/1738-494x(Print)/1976-3824(Online)
DOI 10.1007/s12206-019-0232-2

Tooth friction force and transmission error of spur gears due to sliding friction †

Chan IL Park*

Department of Precision Mechanical Engineering, Gangneung-Wonju National University, Wonju 26403, Korea

(Manuscript Received August 19, 2018; Revised November 2, 2018; Accepted November 8, 2018)

Abstract

This study investigated the tooth friction force and transmission error (TE) of spur gears due to sliding friction under quasi-static condition. The sliding velocity and friction force of spur gears and mesh compliance during meshing were calculated. The load–deformation relations between the tooth normal load, tooth errors, and mesh compliance, and moment equilibrium equation, including friction force, were derived. The friction force, tooth load, and TE of unmodified and linear tip-relief modified spur gears were analyzed by using the derived equations. Results indicated that the friction force, tooth load, and TE increased during approach and decreased in recess regardless of tooth modification, particularly in the single-mesh region. Friction caused larger peak-to-peak change of TE than that without friction. Xu's friction coefficient generated smooth TE and tooth load transitions near the pitch point, and BK's friction coefficient remained approximately constant, except for the sharp increase in tooth load and TE near the pitch point.

Keywords: Sliding friction; Spur gear; Friction force; Tooth load; Transmission error

1. Introduction

Efficiency of gears must be improved to meet the regulations regarding CO_2 and fuel economy. Frictional mechanics of spur gears as the basic gear should be investigated to improve the efficiency of gears. Tavakoli and Houser [1] developed a procedure to calculate the static transmission error (TE) and tooth load of spur gears without considering the friction force. Kar and Mohanty [2, 3] determined the time-varying contact length and computed the friction force of helical gears. Vaishya and Singh [4] estimated the frictional force and applied sliding friction to several gear dynamic models. He et al. analytically investigated the effect of tooth-profile modification in spur gears with sliding friction on dynamic transmission error (DTE) [5] and predicted the friction forces by using several sliding friction formulations [6]. Park analyzed the tooth load and TE of spur gears with constant friction coefficient [7]. Liu et al. [8] reported the production of additional DTE vibration magnitude due to the sliding friction of spur gears during meshing without detailed TE analysis. Han et al. [9] calculated the mesh stiffness of helical gears with consideration of friction. However, the comprehensive tooth load and TE analysis of spur gears under real friction coefficient were not investigated. Friction of spur gears generates heat, which results in the increase of lubricant temperature and decrease of viscosity. The decrease in viscosity increases friction due to the increase of metal-to-metal contact, which reduces efficiency. Therefore, friction is related to surface roughness, lubrication, temperature, torque, and gear kinematics. The friction force of spur gears at the pitch point changes the direction. Frictional force generates vibration due to its reverse direction during meshing. The bearings and housing load are accurately calculated by friction forces. Tooth friction is remarkable at a high torque and low speed.

In this study, the kinematic relationship on the sliding velocity of spur gears and compliance is investigated. The load-deformation relations between the tooth normal load, TE, and mesh compliance, and the moment equilibrium, including the friction force, are derived. The TE, tooth load, and tooth sliding friction forces are calculated by using the derived equations. The effects of constant/variable friction coefficient on unmodified and linear tip-relief modified spur gears are evaluated.

2. Friction force-related equations

Sliding friction force of spur gears acts against sliding velocity, which has different directions during approach and recess actions. Friction force is associated with gear–mesh kinematics, and is derived for approach and recess actions. Load-deformation equations and moment equilibrium with friction force are derived to obtain the TE. Spur gears are assumed to have a low contact ratio.

*Corresponding author. Tel.: +82 33 760 8723, Fax.: +82 33 760 8721
E-mail address: pci@gwnu.ac.kr
† Recommended by Associate Editor Ki-Hoon Shin

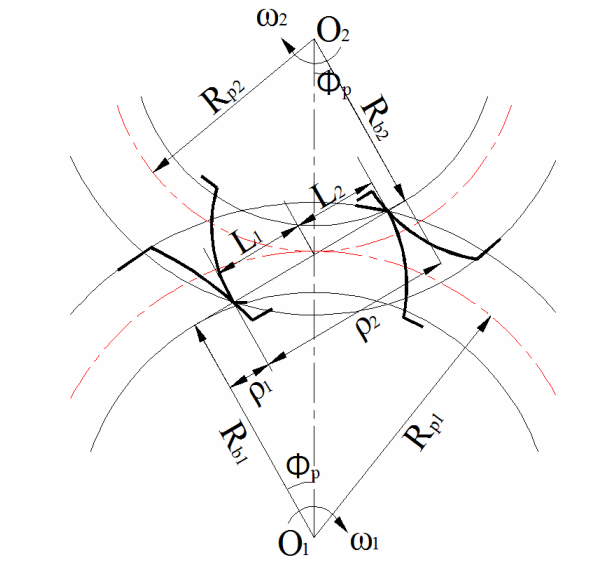

Fig. 1. Meshing kinematics of involute spur gear.

2.1 Sliding velocity and friction force in approach

Gear–mesh is composed of approach and recess actions. In this section, the sliding velocity and friction force for approach are derived. The radius of curvature in Fig. 1 when the gear approaches from initial meshing to the pitch point is derived as follows [10]:

$$\rho_1 = R_{p1}\sin\varphi_p - L_1, \tag{1a}$$

$$\rho_2 = R_{p2}\sin\varphi_p + L_1. \tag{1b}$$

where L_1 is the distance from the pitch point to the meshing point along the line of action and changes from 0 to L_a:

$0 < L_1 \le L_a$, $L_a = \sqrt{R_{o2}^2 - R_{b2}^2} - R_{p2}\sin\varphi_p$.

The rolling velocities of driving and driven gears are expressed as

$$V_1 = \rho_1\omega_1, \tag{2a}$$

$$V_2 = \rho_2\omega_2. \tag{2b}$$

Sliding velocity is determined as

$$V_s = V_1 - V_2 = \rho_1\omega_1 - \rho_2\omega_2. \tag{3}$$

The sliding velocity when the relation of constant pitch velocity and Eq. (1) are applied to Eq. (3) is expressed as follows:

$$V_S = -L_1(\omega_1 + \omega_2). \tag{4}$$

The friction force in approach is directed toward the gear center in the off-line direction of action due to the negative sliding velocity of Eq. (4). A normal load and a friction force, which is the product of friction coefficient and normal load by applying the moment equilibrium about the gear center are expressed as [7]:

$$W_n = \frac{T_1}{R_{b1}(1-\mu\tan\theta)}, \tag{5a}$$

$$W_f = \frac{\mu T_1}{R_{b1}(1-\mu\tan\theta)}. \tag{5b}$$

2.2 Sliding velocity and friction force in recess

To calculate the friction force in recess, the radius of curvature in recess is derived as follows:

$$\rho_1 = R_{p1}\sin\varphi_p + L_2, \tag{6a}$$

$$\rho_2 = R_{p2}\sin\varphi_p - L_2. \tag{6b}$$

where L_2 is the distance from the pitch point to the meshing point along the line of action and varies from 0 to L_r:

$0 < L_2 \le L_r$, $L_r = \sqrt{R_{o1}^2 - R_{b1}^2} - R_{p1}\sin\varphi_p$.

The positive sliding velocity by using a similar manner to approach is obtained as follows:

$$V_s = V_1 - V_2 = L_2(\omega_1 + \omega_2). \tag{7}$$

Compared with approach, the friction force when the contact is on recess acts on opposite direction from the gear center in the off-line direction of action. A normal load and a friction force by applying the moment equilibrium about the gear center are expressed as [7]:

$$W_n = \frac{T_1}{R_{b1}(1+\mu\tan\theta)}, \tag{8a}$$

$$W_f = \frac{\mu T_1}{R_{b1}(1+\mu\tan\theta)}. \tag{8b}$$

2.3 Compliance

Tooth deflection consists of bending and shear, Hertzian-type contact, and tooth-foundation deflections. A spur gear tooth is modeled as a non-uniform cantilever beam with an effective length to obtain bending and shear deflections. The tooth displacement in the direction of the applied normal load is calculated based on cantilever beam theory under the assumption of fixed tooth on a rigid foundation. Bending and shear compliance at the j^{th} calculation point are given as follows [11]:

$$Q_{bj} = \sum_k \frac{1}{E\bar{I}_k}[\cos^2\theta(L_k^3 + 3S_{jk}L_k^2 + S_{jk}^2L_k)/3 - \cos\theta\sin\theta Y_j (L_k^2 + 2S_{jk}L_k) + \sin^2\theta Y_j^2 L_k], \tag{9}$$

$$Q_{sj} = \sum_k \frac{1.2L_k\cos^2\theta}{G\bar{A}_k}. \tag{10}$$

A modified version of Palmgren's equation is used for a simple calculation of contact compliance, which is expressed as follows [1, 11]:

$$Q_h = \frac{1.37}{E_{e12}^{0.9} F^{0.8} W_n^{0.1}}, \tag{11}$$

where the combined effective Young's modulus is $E_{e12} = \frac{2E_{e1}E_{e2}}{E_{e1}+E_{e2}}$.

Foundation compliance is used to eliminate the previous rigid foundation assumption [1, 12]. Considering that a narrow tooth is supported by plane stress theory, foundation compliance at the loading position is expressed as

$$Q_{fj} = \frac{\cos^2\theta}{F \cdot E_e}\left[\frac{16.67}{\pi}\left(\frac{L_f}{H_f}\right)^2 + 2(1-\upsilon)\cdot\left(\frac{L_f}{H_f}\right) + 1.534\left(1+\frac{Tan^2\theta}{2.4(1+\upsilon)}\right)\right]\cdot \tag{12a}$$

Considering that plane strain theory prevails for a wide tooth, foundation compliance is expressed as

$$Q_{fj} = \frac{\cos^2\theta}{F \cdot E_e}(1-\upsilon^2)\left[\frac{16.67}{\pi}\left(\frac{L_f}{H_f}\right)^2 + 2\left(\frac{1-\upsilon-2\upsilon^2}{1-\upsilon^2}\right)\cdot\left(\frac{L_f}{H_f}\right) + 1.534\left(1+\frac{Tan^2\theta}{2.4(1+\upsilon)}\right)\right]. \tag{12b}$$

The total tooth compliance at the j^{th} calculation point is obtained based on the sum of bending, shear, contact, and foundation compliance, which is expressed as follows:

$$Q_{j12} = Q_{bj12} + Q_{sj12} + Q_{fj12} + Q_h. \tag{13}$$

2.4 Moment equilibrium and load-deformation equation

Spur gears are assumed to have one or two pairs of teeth mesh to derive the TE equations and tooth load of spur gears. The normal load and friction forces of driving gear in two pairs of meshing teeth are shown in Fig. 2. The load across the face width of gears is assumed to be uniformly distributed. The load-deformation relations with tooth modification and profile errors, tooth compliance, and tooth normal load, and the moment equilibrium with input torque, friction forces, and normal load yield at the j^{th} calculation point are expressed in the three following equations:

$$\Delta_j + W_{nj}^1 Q_j^1 = E_j^1, \tag{14}$$

$$\Delta_j + W_{nj}^2 Q_j^2 = E_j^2, \tag{15}$$

$$W_{nj}^2 R_{b1} + W_{nj}^1 R_{b1} - \mu^2 W_{nj}^2 \rho_j^2 + \mu^1 W_{nj}^1 \rho_j^1 = T_1. \tag{16}$$

The TE and tooth load are determined by solving simultaneous equations. In two pairs of meshing teeth, the TE and

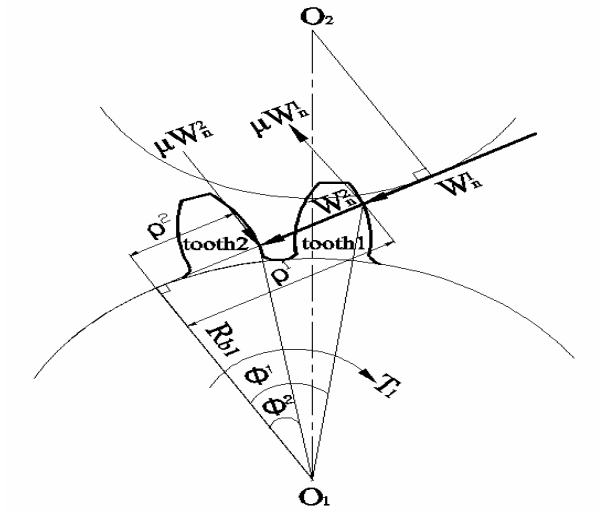

Fig. 2. Forces acting in two pairs of meshing teeth.

normal load of the first and second meshing teeth at the j^{th} calculation point are expressed as follows:

$$\Delta_j = \frac{T_1 Q_j^1 Q_j^2 + E_j^2\left(R_{b1} - \mu^2\rho_j^2\right)Q_j^1 + E_j^1\left(R_{b1} + \mu^1\rho_j^1\right)Q_j^2}{R_{b1}\left(Q_j^1 + Q_j^2\right) + \left(\mu^1\rho_j^1 Q_j^2 - \mu^2\rho_j^2 Q_j^1\right)}. \tag{17}$$

$$W_{nj}^1 = \frac{T_1 Q_j^2 + \left(E_j^1 - E_j^2\right)\left(R_{b1} - \mu^2\rho_j^2\right)}{R_{b1}\left(Q_j^1 + Q_j^2\right) + \left(\mu^1\rho_j^1 Q_j^2 - \mu^2\rho_j^2 Q_j^1\right)}, \tag{18}$$

$$W_{nj}^2 = \frac{T_1 Q_j^1 + \left(E_j^2 - E_j^1\right)\left(R_{b1} + \mu^1\rho_j^1\right)}{R_{b1}\left(Q_j^1 + Q_j^2\right) + \left(\mu^1\rho_j^1 Q_j^2 - \mu^2\rho_j^2 Q_j^1\right)}. \tag{19}$$

The force of tooth 1 is tensile when tooth load 1 of Eq. (18) is negative. Tooth 1 loses meshing, and only tooth 2 is in a meshing state. Then, the normal load and TE are expressed as follows:

$$W_{nj}^1 = 0, \tag{20}$$

$$W_{nj}^2 = T_1 / \left(R_{b1} - \mu^2\rho_j^2\right), \tag{21}$$

$$\Delta_j = E_j^2 - W_{nj}^2 Q_j^2. \tag{22}$$

By contrast, tooth 2 loses meshing, and only tooth 1 is in a meshing state when tooth load 2 of Eq. (19) is negative. In this case, the normal load and TE are expressed as follows:

$$W_{nj}^2 = 0, \tag{23}$$

$$W_{nj}^1 = T_1 / \left(R_{b1} + \mu^1\rho_j^1\right), \tag{24}$$

$$\Delta_j = E_j^1 - W_{nj}^1 Q_j^1. \tag{25}$$

The sliding friction forces are obtained by multiplying the friction coefficients and the normal load.

Table 1. Spur gear specification.

	Pinion	Gear
Number of teeth	30	26
Face width (mm)	16	13
Outside diameter (mm)	65.7	57.9
Pitch diameter (mm)	60	52
Addendum mod. co.	0.57	0.55
Normal module	2	-
Normal pressure angle (°)	20°	-
Center distance (mm)	58	-
Whole depth (mm)	4.26	-

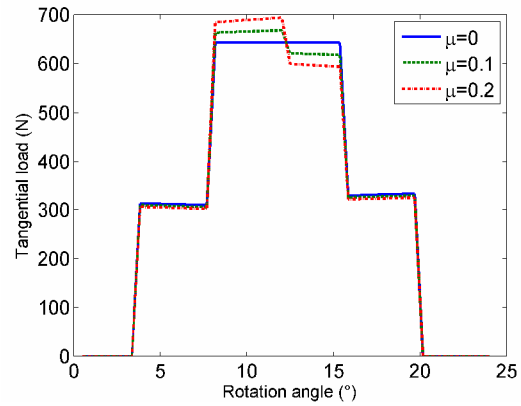

Fig. 3. Tangential load of unmodified gears.

3. Results and discussion

3.1 Constant friction coefficient

The TE and tooth load of unmodified and tip relief modified spur gears with constant friction coefficient are calculated based on the spur gear data of Table 1, input torque of 20 N·m, and steel material (Young's modulus = 206 GPa, Poisson's ratio = 0.29). A constant friction coefficient of 0.1 provides good results at a low speed in mixed or boundary lubrication regimes, and a constant friction coefficient of 0.05 yields satisfactory results at a high speed in hydrodynamic lubrication regimes [13]. The driving and driven teeth are assumed to have the same constant friction coefficient ($\mu^1 = \mu^2$)in investigating the effect of constant friction coefficient. An analysis is conducted under $4\pi / z_1$ with an angle increment of $2\pi / 25z_1$.

The unmodified gears are analyzed on three friction coefficients of 0 (no friction), 0.1 and 0.2. Fig. 3 shows that the tangential load on a driving gear tooth changes with the rolling of gears. The tooth load increases during approach and decreases during recess due to friction. The magnitude is obvious in the single-mesh region and increases due to high friction coefficient.

The sliding friction force of driving gear tooth has a stair shape in the single and double-mesh regions, as shown in Fig. 4. The friction force changes at the pitch point from negative

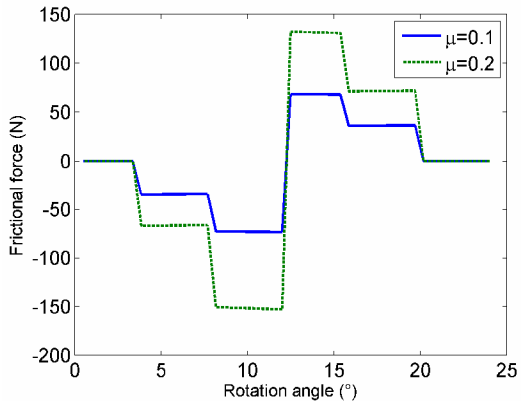

Fig. 4. Sliding friction force of unmodified gears.

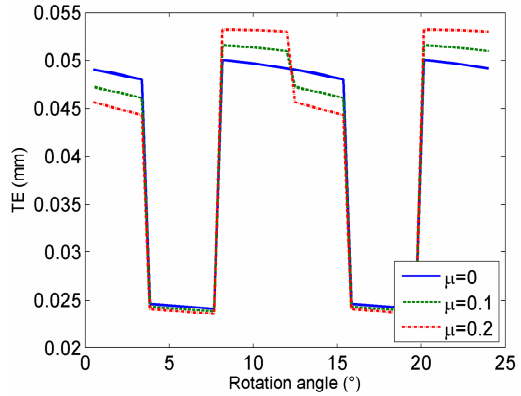

Fig. 5. TE of unmodified gears.

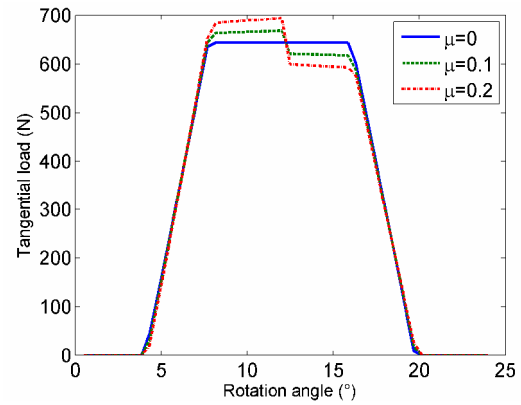

Fig. 6. Tangential load of tip-relief modified gears.

to positive, which indicates a change of direction. Fig. 5 shows the absolute magnitude of TE at roll angle of 24°, which starts meshing from the pitch point. The TE increases during approach and decreases during recess due to friction, which are particularly remarkable in the single-mesh region. This condition is similar to the DTE reported by He [5]. Friction causes larger peak-to-peak change of TE than that without friction, which indicates the increase of gear noise.

Spur gears with linear tip-relief modification are analyzed based on three coefficients of friction, namely, 0, 0.1 and 0.2.

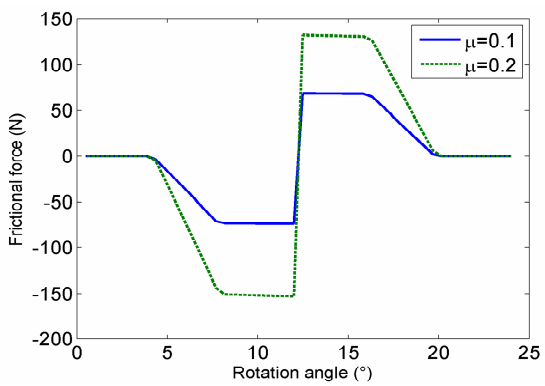

Fig. 7. Sliding friction force of tip-relief modified gears.

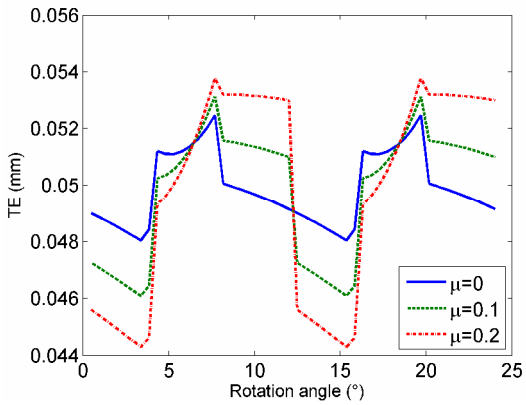

Fig. 8. TE of tip-relief modified gears.

The amount of linear tip relief uses the maximum TE of unmodified spur gears, and the extent of modification is from the highest-point single-tooth contact to the tip.

Linear tip relief modification transforms a stair-shaped tangential load into a smooth tangential load in the double mesh region, as shown in Fig. 6. The tangential load increases during approach and decreases during recess in the single-mesh region due to friction.

Friction force gradually changes in the double-mesh region and reverses at the pitch point. The friction force increases in the single mesh with the increase of friction coefficient, as shown in Fig. 7.

The absolute magnitude of the TE of tip-relief modified gears differs from that of unmodified gears shown in Fig. 5. The magnitude of the TE in tip-relief modified gears increases during approach and decreases during recess due to friction. Friction yields the TE with a different shape and results in less fluctuation than that of unmodified gears, as shown in Fig. 8. Similar to unmodified gears, friction produces more remarkable change of TE than that without friction.

3.2 Variable friction coefficient

A previous analysis assumed that gears have a constant friction coefficient. However, gears have a variable friction coefficient during meshing due to the sliding velocity and changes in lubrication conditions between the meshing teeth. Martin reviewed the rolling and sliding friction effects of gears in mixed and electrohydrodynamic regimes [14]. Benedict and Kelley (BK) [15] suggested an empirical equation for variable friction coefficient under mixed lubrication based on the curve fitting of friction measurements by using a roller test machine. Rebbechi et al. [16] performed dynamic friction force measurements on spur gear teeth and reported that the BK equation agrees well with the measurements, except at meshing positions close to the pitch point. Xu proposed a coefficient of friction and predicted the mechanical efficiency of gear pairs by using the proposed friction coefficient [17, 18]. Matsumoto and Morikawa introduced a friction coefficient for a mixed lubrication condition by using the maximum height of surface roughness rather than the average surface roughness [19]. Representative BK's [15] and Xu's coefficients [17] were employed among the proposed variable friction coefficients. A modified empirical equation of BK in terms of average tooth surface roughness (S_{avg}) and in accordance with the International System of Units is given as follows [6, 15]:

$$\mu_{Bi} = \frac{0.0127 \times 1.13}{1.13 - S_{avg}} \cdot \log_{10}\left[\frac{29662 w_n}{\eta_o V_{si} V_{ei}^2}\right], \tag{26}$$

where $w_n = T_1 / (F \cdot R_{p1} \cos\varphi_p)$ and $S_{avg} = 0.5(S_1 + S_2)$. The sliding and entraining velocities of the ith meshing tooth pair are given by $V_{si}(t) = \left|V_{1i}(t) - V_{2i}(t)\right|$ and $V_{ei}(t) = \left|V_{1i}(t) + V_{2i}(t)\right|$, respectively, where i = 1, 2…

Xu et al. [17, 18] proposed a friction formula with zero friction coefficient at the pitch point. The formula was obtained by using the non-Newtonian, thermal elastohydraulic lubrication formulation as follows:

$$\mu_{Xi}(t) = e^{f(SR_i(t), P_{hi}(t), \eta_o, S_{avg})} P_{hi}^{b_2} \left|SR_i(t)\right|^{b_3} V_{eim}^{b_6}(t) \eta_o^{b_7} \rho_i^{b_8}(t), \tag{27a}$$

$$f(SR_i(t), P_{hi}(t), \eta_o, S_{avg}) = b_1 + b_4 \left|SR_i(t)\right| P_{hi}(t) \log_{10}(\eta_o) + b_5 e^{-\left|SR_i(t)\right| P_{hi}(t) \log_{10}(\eta_o)} + b_9 e^{S_{avg}}. \tag{27b}$$

The empirical constant coefficients for the above formula are given as follows: $b_1 = -8.92$, $b_2 = 1.03$, $b_3 = 1.04$, $b_4 = -0.35$, $b_5 = 2.81$, $b_6 = -0.10$, $b_7 = 0.75$, $b_8 = -0.39$ and $b_9 = 0.62$. The composite relative radius of curvature $\rho_i(t)$ of the i^{th} meshing tooth pair is given by $\rho_i(t) = \frac{\rho_{1i}(t)\rho_{2i}(t)}{\rho_{1i}(t) + \rho_{2i}(t)}$, $i = 1, 2$. The maximum Hertzian pressure (GPa) for the i^{th} meshing tooth pair is given by $P_{hi}(t) = \sqrt{\frac{w_n E_{e12}}{2\pi\rho_i(t)}}$, $i = 1, 2$. Dimensionless slide-to-roll ratio $SR_i(t)$ and oil entraining velocity $V_{eim}(t)$ of the i^{th} meshing tooth pair are defined as follows:

$$SR_i(t) = \frac{2V_{si}(t)}{V_{ei}(t)}, \quad V_{eim}(t) = \frac{V_{ei}(t)}{2}, i = 1, 2, ..$$

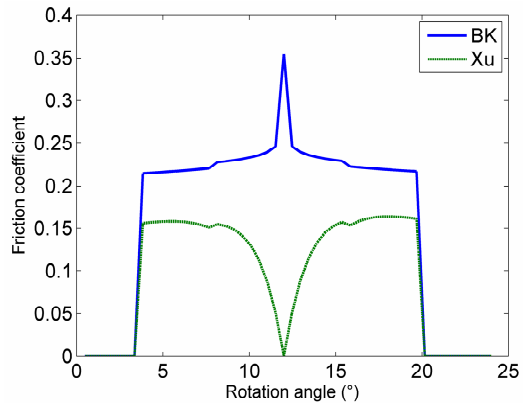

Fig. 9. Friction coefficients of unmodified gears obtained based on BK's and Xu's equations.

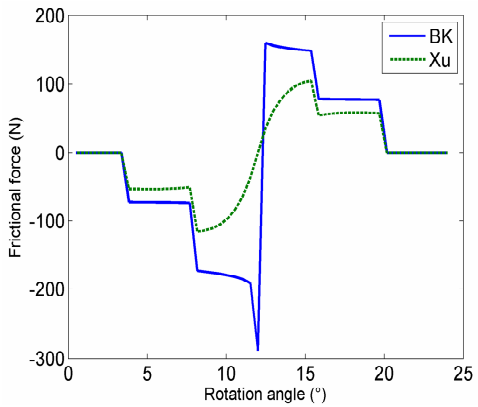

Fig. 11. Sliding frictional force of unmodified gears obtained based on BK's and Xu's equations.

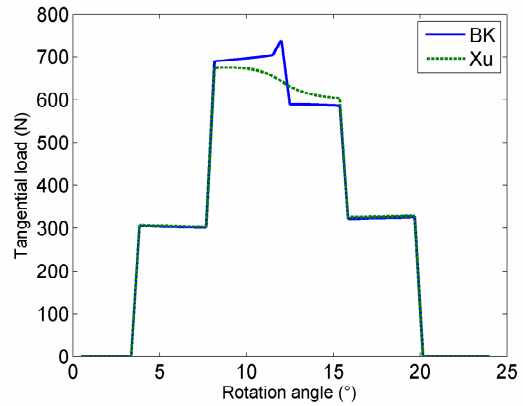

Fig. 10. Tangential load of unmodified gears obtained based on BK's and Xu's equations.

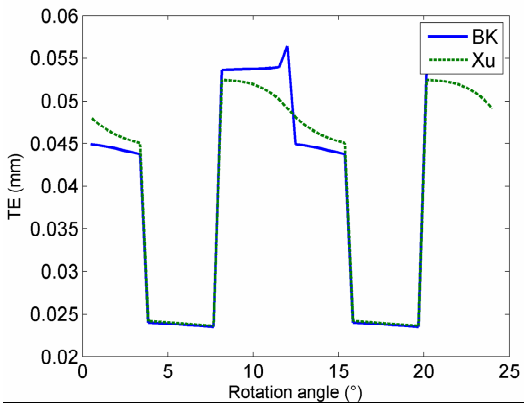

Fig. 12. TE of unmodified gears obtained based on BK's and Xu's equations.

Fig. 9 shows BK's and Xu's friction coefficients for unmodified gears rolling at 3 rpm. For the application of BK's friction coefficient, the tooth surface roughness is 0.4 μm, and the lubricant absolute viscosity is 82 mPa·s. BK's friction coefficient is higher than that of Xu's friction coefficient. However, BK's and Xu's coefficients are remarkably reduced and have an approximate value of 0.1 at 300 rpm, except at the pitch point. BK's coefficient remarkably increases, and Xu's coefficient sharply decreases at the pitch point, whereas the two coefficients remain similar at positions far from the pitch point. The tooth load, friction force, and TE use the friction coefficient at 3 rpm to obtain the quasi-static effect.

Fig. 10 shows the tangential load of unmodified gears when BK's and Xu's friction coefficients are applied. BK's friction coefficient causes a sharp increase in the tangential load at the pitch point and exhibits the same trend with the constant friction coefficient at positions far from the pitch point. Xu's coefficient produces a smooth transition from approach to recess, whereas the constant friction coefficient exhibits a stepped decrease from approach to recess. BK's friction coefficient sharply increases the stepped friction force of unmodified gears at the pitch point, and Xu's coefficient yields a smooth transition from a negative frictional force to a positive friction force, as shown in Fig. 11.

BK's friction coefficient is approximately constant, except for a sharp increase in the TE at the pitch point between the increased TE at approach and decreased TE at recess, and Xu's coefficient yields a smooth transition between the increased TE at approach and decreased TE at recess, as shown in Fig. 12.

Fig. 13 shows BK's and Xu's friction coefficients for tip-relief modified gears operating at 3 rpm. Similar to unmodified gears, BK's friction coefficient is higher than that of Xu's friction coefficient. BK's friction coefficient for tip-relief modified gears remarkably increases at the pitch point but has a slightly different shape from that for unmodified gears at positions far from the pitch point. Xu's friction coefficient is similar between tip-relief modified and unmodified gears.

For tip-relief modified gears, BK's friction coefficient causes a sharp increase in the tangential load at the pitch point, with an increase in the tangential load at approach and a decrease in the tangential load at recess. Xu's friction coefficient yields a smooth transition of the tangential load from approach to recess, as shown in Fig. 14.

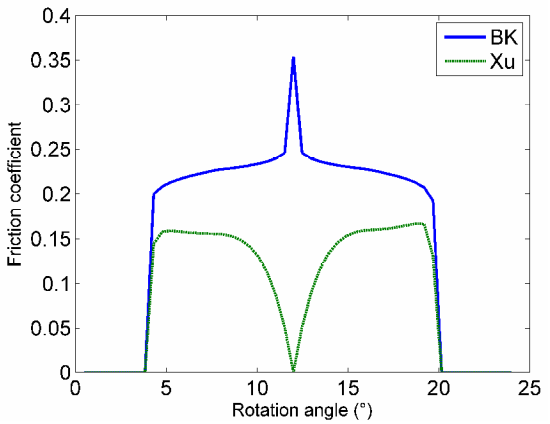

Fig. 13. BK's and Xu's friction coefficients for tip-relief modified gears.

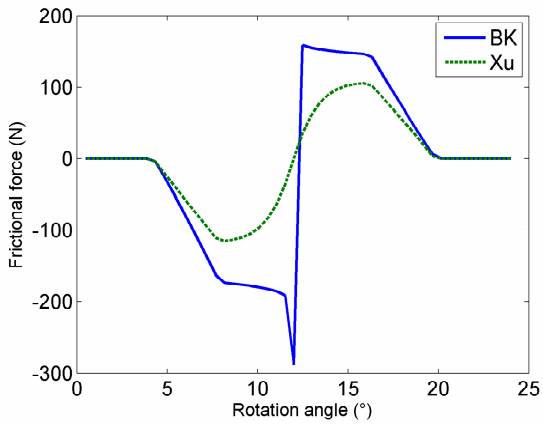

Fig. 15. Sliding frictional force of tip-relief modified gears obtained based on BK's and Xu's equations.

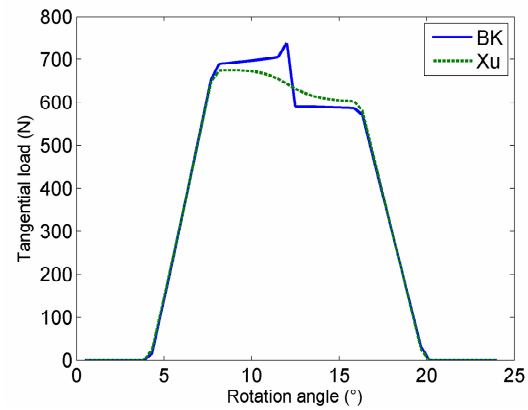

Fig. 14. Tangential load of tip-relief modified gears based on BK's and Xu's equations.

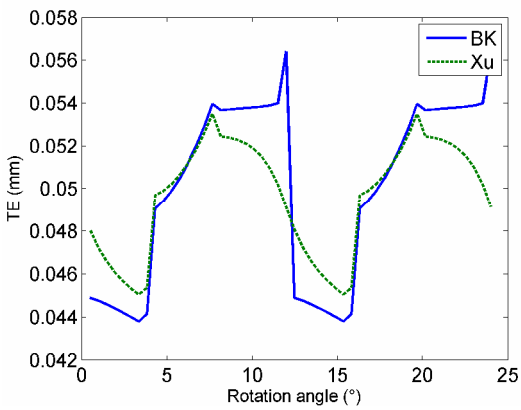

Fig. 16. TE of tip-relief modified gears obtained based on BK's and Xu's equations.

BK's friction coefficient makes the smooth friction force with the peak at the pitch point different from the stepped frictional force of unmodified gears, and Xu's coefficient yields a smooth transition from a negative friction force to a positive frictional force, as shown in Fig. 15. Similarly, BK's coefficient is approximately constant, except for a sharp increase in the TE at the pitch point, and Xu's yields a smooth transition of the TE near the pitch point, as shown in Fig. 16. In summary, BK's friction coefficient is approximately constant, except for the sharp increase in tangential load, friction force, and TE near the pitch point. Meanwhile, Xu's yields a smooth transition near the pitch point. Thus, Xu's friction coefficient appears to be acceptable because the pitch point has no sliding friction.

4. Conclusions

In this study, the friction force, tooth load, and TE of spur gears due to sliding friction in quasi-static condition were investigated. On this basis, the moment equilibrium and load-deformation equations of spur gears with a low contact ratio were derived. The TE, tooth load, and friction force of unmodified and linear tip-relief modified gears with the constant/variable friction coefficient were analyzed by using the derived equations. The conclusions based on the analysis are summarized as follows:

(1) The friction force, tooth load, and TE increased in approach and decreased in recess due to sliding friction. The friction caused larger peak-to-peak change of TE than that without friction, which indicates the increase of gear noise.

(2) For unmodified gears with a constant friction coefficient, the friction force changed the magnitude of the stair shape at the pitch point from negative to positive. The magnitude of friction force is particularly remarkable in the single-mesh region and increases due to high friction coefficient.

(3) The linear tip relief modified gear reduced the fluctuation of TE and unmodified gears, and friction produced more remarkable change of TE than that without friction.

(4) Xu's variable friction coefficient yielded a smooth transition of tooth load and TE near the pitch point, and BK's friction coefficient is approximately constant, except for the sharp increase in the tooth load and TE near the pitch point.

Acknowledgments

This research was supported by the Basic Science Research Program through the National Research Foundation of Korea (NRF) funded by the Ministry of Education (NRF-2017R1D1 A3B03032458).

Nomenclature

E : Tooth error
E_e : Effective Young's modulus, Pa
F : Face width, mm
L : Distance along the line of action
Q : Compliance, mm/N
R_p : Pitch radius, mm
R_o : Outside radius, mm
R_b : Base radius, mm
S : Average surface roughness, μm
T : Torque, N·m
V : Velocity, m/s
W : Load, force, N
w_n : Normal load per face width, N/mm
z : Number of teeth
φ_p : Pressure angle at the pitch point
η_o : Absolute viscosity, mPa·s
μ : Friction coefficient
ν : Poisson's ratio
ρ : Radius of curvature, mm
φ : Pressure angle at the contact point
ω : Angular velocity, rad/s
Δ : TE, mm

Subscripts

1 : Driving gear
2 : Driven gear
a : Approach
b : Bending
f : Friction
n : Normal
r : Recess
s : Shear
t : Tangential

Superscripts

1 : Tooth 1
2 : Tooth 2

References

[1] M. S. Tavakoli and D. R. Houser, Optimum profile modifications for the minimization of static transmission errors of spur gears, *ASME J. Mechanisms, Transmissions, and Automation in Design*, 108 (1986) 86-95.

[2] C. Kar and A. R. Mohanty, An algorithm for determination of time-varying frictional force and torque in a helical gear system, *Mech. Mach. Theory*, 42 (2007) 482-496.

[3] C. Kar and A. R. Mohanty, Determination of time-varying contact length, friction force, torque and forces at the bearings in a helical gear system, *J. Sound Vib.*, 309 (2008) 307-319.

[4] M. Vaishya and R. Singh, Strategies for modeling friction in gear dynamics, *ASME J. Mech. Design*, 125 June (2003) 383-393.

[5] S. He, R. Gunda and R. Singh, Effect of sliding friction on the dynamics of spur gear pair with realistic time-varying stiffness, *J. Sound Vib.*, 301 (2007) 927-949.

[6] S. He, S. Cho and R. Singh, Prediction of dynamic friction forces in spur gears using alternate sliding friction formulations, *J. Sound Vib.*, 309 (2008) 843-851.

[7] C. I. Park, Effect of teeth friction on transmission errors and tooth load of spur gears, *Proc. of ASME 2015 Int. Des. Eng. Tech. Conf. & Comput. and Inf. in Eng. Conf., IDETC/CIE 2015,* DETC2015-47048, August 2-5 (2015) Boston, Massachusetts, USA.

[8] F. Liu, H. Jiang, S. Liu and X. Yu, Dynamic behavior analysis of spur gears with constant & variable excitations considering friction influence, *J. Mech. Sci. Tech.*, 30 (12) (2016) 5363-5370.

[9] L. Han, L. Xu and H. Qi, Influences of friction and mesh misalignment on time-varying mesh stiffness of helical gears, *J. Mech. Sci. Tech.*, 31 (7) (2017) 3121-3130.

[10] D. T. Townsend (Eds.), *Dudley's gear Handbook,* 2nd Ed., McGraw-Hill (1992).

[11] J. J. Sciarra, R. W. Howells, J. W. Lenski and R. J. Drago, *Helicopter transmission vibration and noise reduction program*, Vol. II-User's Manual, U.S. Army Research and Technology Laboratories, Report no. USARTL-TR-78-2B, Mar. (1978).

[12] R. W. Cornell, Compliance and stress sensitivity of spur gear teeth, *ASME J. Mech. Design*, 103 April (1981) 447-459.

[13] Y. Diab, F. Ville and P. Velex, Prediction of power losses due to tooth friction in gears, *Tribology Transactions*, 49 (2006) 260-270.

[14] K. F. Martin, A review of friction predictions in gear teeth, *Wear*, 49 (1978) 201-238.

[15] G. H. Benedict and B. W. Kelley, Instantaneous coefficients of gear tooth friction, *Trans. of the American Society of Lubrication Engineers*, 4 (1961) 59-70.

[16] B. Rebbechi, F. B. Oswald and D. P. Townsend, Measurement of gear tooth dynamic friction, *ASME Power Transmission and Gearing Conf. Proc.*, DE-Vol. 88 (1996) 355-363.

[17] H. Xu, Development of a generalized mechanical efficiency prediction methodology, *Ph.D Dissertation*, The Ohio State University (2005).

[18] H. Xu, A. Kahraman, N. E. Anderson and D. G. Maddock, Prediction of mechanical efficiency of parallel-axis gear

pairs, *ASME J. Mech. Design*, 129 (1) (2007) 58-68.
[19] S. Matsumoto and K. Morikawa, The new estimation formula of coefficient of friction in rolling-sliding contact surface under mixed lubrication condition for the power loss reduction of power transmission gears, *Proc. of Int. Gearing Conf.*, Lyon, France (2014) II, 1078-1088.

Chan IL Park received his B.S., M.S., and Ph.D. in mechanical engineering at Seoul National University and worked at Hyundai Motor Company for eight years. He served as a Dean of the College of Engineering at Kangnung National University for two years. He is the President of KSME and a Professor in the precision mechanical engineering at Gangneung–Wonju National University. His research interests include gears, plate, shell, optimal design, noise, and vibration.